Insertion of Strongly Electron Withdrawing Cyanoolefins into the C−H Bond in Pentamethylcyclopentadienyl−Rhodium(III) and −Iridium(III) Complexes Containing P−O or P−O−O′ Coordinations

Yasuhiro Yamamoto,*,† Xiao-Hong Han,† Saho Nishimura,†
Ken-ichiro Sugawara,† Nobumichi Nezu,† and Tomoaki Tanase‡,§

Department of Chemistry, Faculty of Science, Toho University, Miyama, Funabashi, Chiba, 274-8510 Japan, and Department of Chemistry, Faculty of Science, Nara Women's University, Kitauoya-Higashimachi, Nara, 630-8285 Japan

Received September 12, 2000

Complexes, Cp*MCl(MDMPP-*P,O*) (**1a**: M = Rh, **1b**: M = Ir; Cp* = η^5-C_5Me_5; MDMPP-*P,O* = *P*$Ph_2(C_6H_3$-2-*O*-6-MeO)) readily react with tcne or tcnq to form the 1:1 adducts [Cp*MCl(MDMPP-*P,O*)(ol)] (ol = tcne (**c**), tcnq (**d**)) (**3ac**: M = Rh, ol = tcne; **3bc**: M = Ir, ol = tcne; **4ad**: M = Rh, ol = tcnq; **4bd**: M = Ir, ol = tcnq), derived from insertion of cyanoolefins into the C−H bond adjacent to the metal−O bond. Complex Cp*Ir(TDMPP-*P,O,O′*) **2b** (TDMPP-*P,O,O′* = P{C_6H_3-2,6-$(MeO)_2$}(C_6H_3-2-*O*-6-MeO$)_2$) bearing a (P,O,O′) coordination was treated with 1 equiv of tcne, tcnq, or Me_2-tcnq (**e**) to give the products in which one molecule of cyanoolefin was inserted, [Cp*Ir(TDMPP-*P,O,O′*)(ol)] (**5bc**: ol = tcne; **6bd**: ol = tcnq; **6be**: ol = Me_2-tcnq). Reactions with 2 equiv of cyanoolefin gave the products [Cp*Ir(TDMPP-*P,O,O′*)$(ol)_2$] (**7bc**: ol = tcne; **8bd**: ol = tcnq), in which insertion occurred at two C−H positions adjacent to the Ir−O bonds. Structural data for **3ac**, **3bc**, **4ad**, **5bc**, and **7bc** are described.

Introduction

Aromatic phosphines bearing methoxy groups at the 2- and 6-positions of the phenyl groups exhibit high basicity and nucleophilicity.[1−3] Recently we reported that one or two of the *ortho*-methoxy groups in (2,6-dimethoxyphenyl)diphenylphosphine (MDMPP), bis(2,6-dimethoxyphenyl) phenylphosphine (BDMPP), and tris-(2,6-dimethoxyphenyl)phenylphosphine (TDMPP) were demethylated in the reactions with bis[dichloro(η^6-arene)ruthenium(II)] or bis[dichloro(η^5-pentamethylcyclopentadienyl)rhodium(III) (or iridium(III))] to give (η^6-arene)RuCl(MDMPP-*P,O*), (η^6-arene)RuCl(TDMPP-*P,O*)[4] (arene = *p*-cymene, 1,2,3-$Me_3C_6H_3$, 1,3,5-$Me_3C_6H_3$, and C_6Me_6), Cp*MCl(MDMPP-*P,O*), Cp*MCl(BDMPP-*P,O*), and Cp*M(TDMPP-*P,O,O′*) (M = Rh[5] and Ir;[6] Cp* = η^5-C_5Me_5; MDMPP-*P,O* = $PPh_2(C_6H_3$-2-*O*-6-MeO), BDMPP-*P,O* = *P*Ph{C_6H_3-2,6-$(MeO)_6$}(C_6H_3-2-*O*-6-MeO), TDMPP-*P,O,O′* = *P*{C_6H_3-2,6-$(MeO)_6$}(C_6H_3-2-*O*-6-MeO$)_2$) with (*P,O*) or (*P,O,O′*) chelating phosphines, respectively. When complexes Cp*MCl(MDMPP-*P,O*) (**1a**: M = Rh; **1b**: M = Ir) were treated with 1-alkyne or disubstituted alkyne in the presence of KPF_6 or $NaPF_6$, novel single or double insertion of alkyne into the Rh−O or P−C bond gave six- or seven-membered metallacycles.[7,8] Reaction of Cp*RhCl(BDMPP-*P,O*) with HC≡CC_6H_4-4-R (R = COOMe, NO_2) underwent unprecedented transannular addition between the rhodium atom and *ipso*-carbon atom of the phenyl group of the phosphine ligand.[8]

During the research on interactions of the aforementioned complexes with small molecules such as olefins and alkynes, we found that **1** or Cp*Ir(TDMPP-*P,O,O′*) **2b** (M = Ir) reacted with electron-deficient olefins such as tetracyanoethylene (tcne), 7,7,8,8,-tetracyano-*p*-quinodimethane (tcnq), and 1,5-dimethyl-7,7,8,8-tetracyano-*p*-quinodimethane (Me_2-tcnq) (**e**), which inserted into weakly activated C−H bonds on the phenyl ring of the phosphine ligand. These insertion reactions into a C−H bond on the ligand showed novel reactivity of electron-deficient olefins and are considered as an electrophilic

---

* Corresponding author. Fax: +81-474-75-1855. E-mail: yamamoto@chem.sci.toho-u.ac.jp.
† Toho University.
‡ Nara Women's University.
§ E-mail: tanase@cc.nara-wu.ac.jp.

(1) (a) Wada, M.; Higashimura, A. *J. Chem. Soc., Chem. Commun.* **1984**, 482. (b) Wada, M.; Higashimura, A.; Tsuboi, A. *J. Chem. Res. Synp.* **1985**, 38. Wada, M.; Higashimura, A.; Tsuboi, A. *J. Chem. Res. Miniprint* **1985**, 467.

(2) Wada, M.; Tsuboi, A. *J. Chem. Soc., Perkin Trans.* **1987**, *1*, 151.

(3) (a) Wada, M.; Tsuboi, A.; Nishimura, K.; Erabi, T. *Nippon Kafaku Kaishi* **1987**, 1284. (b) Kurosawa, H.; Tsuboi, A.; Kawasaki, Y.; Wada, M. *Bull. Chem. Soc. Jpn.* **1987**, *60*, 3563.

(4) (a) Yamamoto, Y.; Sato, R.; Ohshima, M.; Matsuo, F.; Sudoh, C. *J. Organomet. Chem.* **1995**, *489*, C68. Yamamoto, Y.; Sato, R.; Matsuo, F.; Sudoh, C.; Igoshi, T. *Inorg. Chem.* **1996**, *35*, 2329. (b) Yamamoto, Y.; Tanase, T.; Sudoh, C.; Turuta, T. *J. Organomet. Chem.* **1998**, *569*, 29.

(5) Han, X.-H.; Yamamoto, Y. *J. Organomet. Chem.* **1998**, *561*, 157.

(6) Yamamoto, Y.; Kawasaki, K.; Nishimura, S. *J. Organomet. Chem.* **1999**, *587*, 49.

(7) Yamamoto, Y.; Han, X.-H.; Ma, J.-F. *Angew. Chem.* **2000**, 113; *Angew. Chem., Int. Ed.* **2000**, *39*, 1965.

(8) Yamamoto, Y.; Sugawara, K. *J. Chem. Soc., Dalton Trans.* **2000**, 2896.

10.1021/om000781c CCC: $20.00

Scheme 1. Reactions of 1 or 2 with Strongly Electron Withdrawing Cyanoolefins

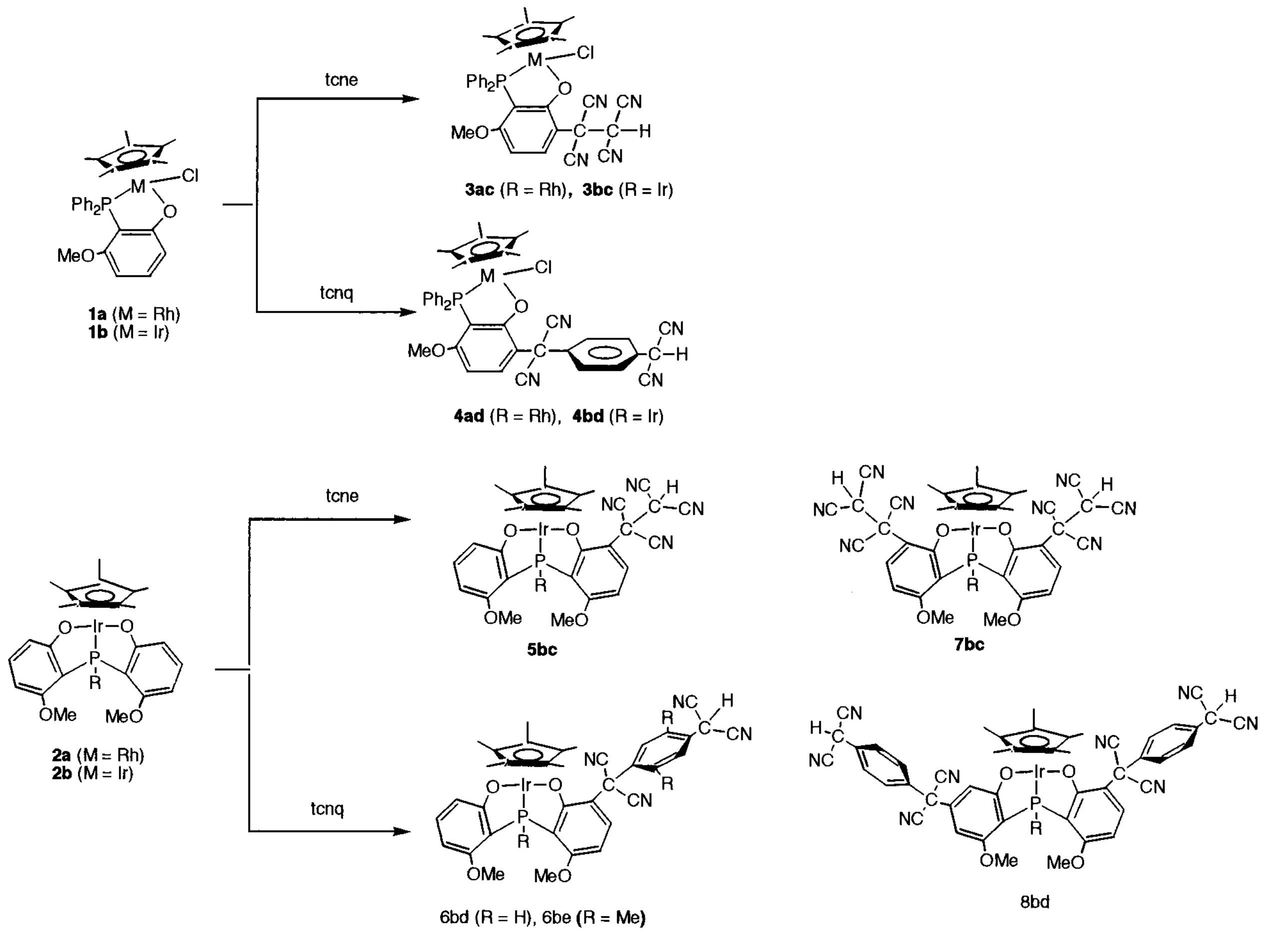

substitution on a weakly activated phenyl ring. Similar insertions of electron-deficient olefins have been documented by Onitsuka et al.: square-planar complexes, 2-furanylplatinum chloride, bearing PMe_3, PEt_3, or PMe_2Ph underwent insertion of tcne or tcnq into the C−H bond at the 3- or 5-position.[9]

A preliminary account of this work has been published.[10]

Results and Discussion

When tcne (**c**) was added to **1a** or **1b** in CH_2Cl_2 at room temperature, the solution became brown or yellow. In each case, the 1:1 adducts, formulated as [Cp*MCl-(MDMPP-*P*,*O*)(tcne)] (**3ac**: M = Rh; **3bc**: M = Ir), were isolated on the basis of fast atom bombardment (FAB) mass spectrometry (Scheme 1). In the IR spectrum of **3ac**, a very weak C≡N stretching frequency appeared at 2250 cm^{-1}, which is higher in energy than those of free tcne (2207 cm^{-1}) and π-complexes (2170−2235 cm^{-1}).[11] However, no infrared signal was observed for **3bc**, as bands in the ν_{CN} region are extremely weak. In the ^1H NMR spectra of **3**, three characteristic resonances around δ 1.50(d), 3.50(s), and 6.40(s) were assigned to the Cp*, methoxy, and $HC(CN)_2$ protons, respectively. The structures of **3ac** and **3bc** were determined by X-ray crystal structure analyses (Figures 1 and 2). Crystallographic data are shown in Table 1. Selected bond lengths and angles are listed in Tables 2 and 3. Complex **3ac** contains a CH_2Cl_2 molecule as a crystal solvent. The tcne molecule was inserted into the C−H bond adjacent to the metal−O σ-bond. The $CH(CN)_2$ and $C(CN)_2R$ groups adopt a staggered conformation, as torsion angles of the C(27)−C(30)−C(31)−C(34) and C(27)−C(30)−C(31)−C(35) bonds are 168.8(5)° and −67.1(6)° for **3ac** and 170.6(7)° and −64.6(8)° for **3bc**,

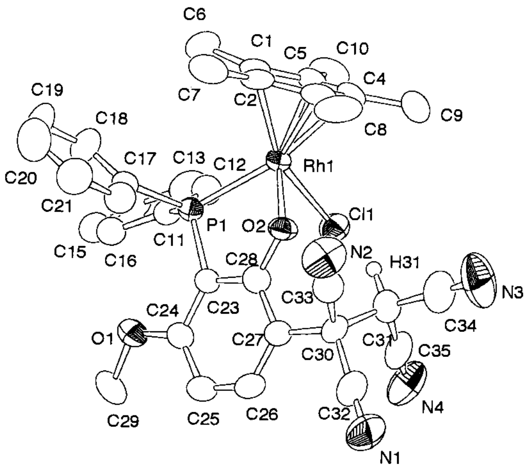

Figure 1. Perspective ORTEP view of the molecular structure of **3ac**·CH_2Cl_2 with thermal ellipsoids drawn at 50% probability. A CH_2Cl_2 molecule was omitted for clarity.

---

(9) Onitsuka, K.; Urayama, H.; Sonogashira, K.; Ozawa, F. *Chem. Lett.* **1995**, 1019.

(10) Yamamoto, Y.; Han, X.-H.; Sugawara, K.; Nishimura, S. *Angew. Chem.* **1999**, *112*, 1318; *Angew. Chem., Int. Ed.* **1999**, *38*, 1242.

(11) For example, Fatiadi, A. J. *Synthesis* **1987**, 959, and references therein.

Table 1. Crystallographic Data for [Cp*RhCl(MDMPP-*P,O*)(tcne)·CH_2Cl_2], 3a·CH_2Cl_2, [Cp*IrCl(MDMPP-*P,O*)(tcne)], 3bc, [(Cp*RhCl(MDMPP-*P,O*)(tcnq)], 4ad, [Cp*Ir(TDMPP-*P,O,O′*)(tcne)], 5bc·H_2O, and [Cp*Ir(TDMPP-*P,O,O′*)(tcne)$_2$], 7bc·0.5CH_2Cl_2

	3ac·CH_2Cl_2	**3bc**	**4ad**	**5bc**·H_2O	**7bc**·0.5CH_2Cl_2
formula	$C_{36}H_{33}N_4O_2PCl_3Rh$	$C_{35}H_{31}N_4O_2PClIr$	$C_{41}H_{35}N_4O_2PClRh$	$C_{38}H_{36}N_4O_6PIr$	$C_{44.5}H_{37}N_8O_6PClIr$
mol wt	793.92	788.3	785.1	867.92	1038.48
cryst syst	monoclinic	monoclinic	monoclinic	monoclinic	monoclinic
space group	$P2_1/c$ (No. 14)	$P2_1/n$ (No. 14)	$P2_1/n$ (No. 14)	$P2_1/c$ (No. 14)	$P2_1/a$ (No. 14)
a, Å	12.047(3)	12.123(5)	13.70(1)	16.601(8)	19.185(4)
b, Å	19.293(3)	14.314(5)	19.076(7)	12.808(6)	11.631(3)
c, Å	16.089(3)	20.407(3)	15.965(10)	18.151(6)	20.056(
β, deg	94.33(2)	95.34(2)	101.31(6)	95.31(3)	95.92(1)
V, $Å^3$	3728(1)	3525(1)	4092(4)	3842(2)	4451(1)
Z	4	4	4	4	4
d(calc), g/cm^3	1.414	1.504	1.274	1.500	1.549
μ, cm^{-1}	7.51	39.53	5.58	35.74	31.60
no. of reflns ($\theta < 50°$)	6790	6485	7450	7099	7784
no. of data used	6551 ($I > -10.0\sigma(I)$)	4487 ($I > 3.0\sigma(I)$)	2941 ($I > 4.0\sigma(I)$)	6747 ($I > -10.0\sigma(I)$)	5378 ($I > 2.0\sigma(I)$)
no. of variables	409	397	397	460	569
R; R_w %	0.122; 0.188[a]	0.028; 0.034[b]	0.055; 0.080[b]	0.162; 0.183[a]	0.048; 0.057[b]
R1 (reflns)	0.065 (4024)			0.061 (3185)	
GOF[c]	1.22	1.33	2.28[b]	0.97	1.38

[a] $R = \sum(F_o^2 - F_c^2)/\sum F_o^2$, $R_w = [\sum w(F_o^2 - F_c^2)^2/\sum w(F_o^2)^2]^{0.5}$ and $R1 = \sum||F_o| - |F_c||/\sum|F_o|$ for $I > 2.0\sigma(I)$. [b] $R = \sum||F_o| - |F_c||/\sum|F_o|$ and $R_w = [\sum w(|F_o| - |F_c|)^2/\sum wF_o^2]^{0.5}$. [c] $GOF = [\sum w(|F_o| - |F_c|)^2/(N_{obs} - N_{parm})]^{1/2}$.

Table 2. Selected Bond Lengths (Å) and Angles (deg) for 3ac·CH_2Cl_2

Rh(1)–Cl(1)	2.412(2)	Rh(1)–P(1)	2.323(2)	Rh(1)–O(2)	2.084(5)
P(1)–C(23)	1.807(8)	C(23)–C(28)	1.399(10)	O(2)–C(28)	1.324(8)
O(1)–C(24)	1.352(9)	C(27)–C(30)	1.51(1)	C(30)–C(31)	1.58(1)
C(30)–C(32)	1.47(1)	C(32)–N(1)	1.13(1)	C(30)–C(33)	1.49(1)
C(33)–N(2)	1.14(1)	C(31)–C(34)	1.45(1)	C(34)–N(3)	1.13(1)
C(31)–C(35)	1.47(1)	C(35)–N(4)	1.14(1)		
Cl(1)–Rh(1)–P(1)	91.31(7)	Cl(1)–Ir(1)–O(2)	84.5(1)	P(1)–Ir(1)–O(2)	80.3(1)
Rh(1)–P(1)–C(23)	99.3(2)	P(1)–C(23)–C(28)	112.4(5)	C(23)–C(28)–O(2)	123.8(7)
Rh(1)–O(2)–C(28)	117.0(4)	C(28)–C(27)–C(30)	117.2(6)	C(27)–C(30)–C(31)	109.5(6)
C(27)–C(30)–C(32)	112.5(7)	C(27)–C(30)–C(33)	112.3(6)	C(31)–C(30)–C(32)	108.5(6)
C(31)–C(30)–C(33)	107.8(7)	C(32)–C(30)–C(33)	106.1(7)	C(30)–C(31)–C(34)	113.4(7)
C(30)–C(31)–C(35)	109.9(7)	C(34)–C(31)–C(35)	110.9(8)	C(30)–C(32)–N(1)	179.5(10)
C(30)–C(33)–N(2)	177.5(9)	C(31)–C(34)–N(3)	177(1)	C(31)–C(35)–N(4)	177(1)

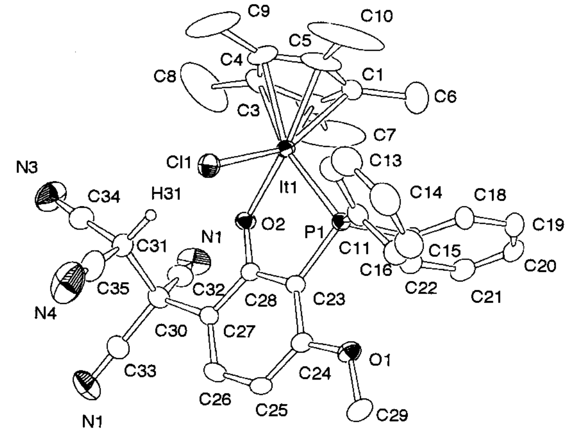

Figure 2. Perspective ORTEP view of the molecular structure of **3bc** with thermal ellipsoids drawn at 50% probability.

respectively. The Rh(1)–P(1), Rh(1)–Cl(1), and Rh(1)–O(1) bond lengths in **3ac** are longer than the corresponding bond lengths of **1a**.[5] The bond distances around the Ir atom in **3bc** are not significantly different from those of **3ac**, but the bond angles are somewhat narrower than those of the rhodium complex. The Cl(1)–M–P(1) angles of 91.3(7)° for **3ac** and of 89.99(5)° for **3bc** are wider than the Cl(1)–M–O(2) and P(1)–M–O(2) bond angles. The C(30)–C(31) bond length is 1.58(1) Å for **3ac** and 1.592(7) Å for **3bc**, respectively, in agreement with a C–C single bond. The Cl(1)···H(31) and Cl(1)···C(31) interatomic contacts are 2.84 and 3.63 Å for **3ac** and 2.78 and 3.63 Å for **3bc**, respectively, suggesting the presence of a very weak Cl···H interaction; this is considered to cause an expansion of the Cl–M–P bond angle and narrowing of the Cl–M–O angle in comparison with those for **1a** (vide infra).

Complexes **1a** and **1b** readily reacted with tcnq (**d**) to form orange crystals formulated as the 1:1 adduct (**4ad** or **4bd**). The IR spectra of **4** showed a C≡N stretching frequency around 2245 cm^{-1}, which is ca. 20 cm^{-1} higher in energy than that for free tcnq. The ^1H NMR spectra showed three characteristic resonances around δ1.40 (d), 3.45 (s), and 5.07 (s), assignable to the Cp*, methoxy, and $HC(CN)_2$ protons, respectively. These chemical shift values appeared at higher fields than those for **3**; this is a result of the strong electron-withdrawing ability of the $C(CN)_2C(CN)_2$ moiety in **3**. The signal for *para*-substituted phenyl protons is an AB-type quartet, suggesting aromatization of the quinone group. The $^{31}P\{^1H\}$ NMR spectra showed a doublet at δ 48.4 (J_{RhP} = 150.0 Hz) for **4ad** and a singlet at δ 28.1 for **4bd**, appearing at higher fields than those for **3**. In the crystal structure analysis of **4ad**, the bulky $C_6H_4C(CN)_2H$ moiety is pointing in the opposite direction as the Cl ligand, different from the cases in **3**, relieving steric repulsion between two groups (Figure 3 and Table 4). The C(30)–C(31) and C(34)–C(37) bond lengths are 1.54(1) and 1.56(1) Å, respectively, in agreement with a C–C single bond. The $C(30)R(CN)_2$ and $C(37)H(CN)_2$

Table 3. Selected Bond Lengths (Å) and Angles (deg) for 3bc

Ir(1)−Cl(1)	2.411(2)	Ir(1)−P(1)	2.311(1)	Ir(1)−O(2)	2.096(3)
P(1)−C(23)	1.813(5)	C(23)−C(28)	1.404(7)	O(2)−C(28)	1.311(6)
O(1)−C(24)	1.352(6)	C(27)−C(30)	1.517(7)	C(30)−C(31)	1.592(7)
C(30)−C(32)	1.494(8)	C(32)−N(1)	1.116(7)	C(30)−C(33)	1.489(8)
C(33)−N(2)	1.127(7)	C(31)−C(34)	1.452(8)	C(34)−N(3)	1.134(8)
C(31)−C(35)	1.450(9)	C(35)−N(4)	1.125(9)		
Cl(1)···H(31)	2.78	Cl(1)···C(31)	3.63		

Cl(1)−Ir(1)−P(1)	89.99(5)	Cl(1)−Ir(1)−O(2)	80.88(10)	P(1)−Ir(1)−O(2)	81.56(9)
Ir(1)−P(1)−C(23)	99.7(2)	P(1)−C(23)−C(28)	113.4(3)	C23−C28−O2	122.3(4)
Ir(1)−O(2)−C(28)	117.9(3)	C(28)−C(27)−C(30)	116.0(4)	C(27)−C(30)−C31	110.1(4()
C(27)−C30−C32	112.0(5)	C(27)−C(30)−C(33)	111.6(4)	C(31)−C(30)−C(32)	107.4(4)
C(31)−C(30)−C(33)	108.7(5)	C(32)−C(30)−C(33)	107.0(5)	C(30)−C(31)−C(34)	112.9(5)
C(30)−C(31)−C(35)	110.1(5)	C(34)−C(31)−C(35)	110.6(5)	C(30)−C(32)−N(1)	176.3(7)
C(30)−C(33)−N(2)	178.3(7)	C(31)−C(34)−N(3)	177.6(8)	C(31)−C(35)−N(4)	177.6(8)

Table 4. Selected Bond Lengths (Å) and Angles (deg) for 4ad

Rh(1)−Cl(1)	2.393(3)	Rh(1)−P(1)	2.306(3)	Rh(1)−O(1)	2.085(7)
P(1)−C(23)	1.800(10)	C(23)−C(24)	1.42(1)	O(1)−C(24)	1.31(1)
O(2)−C(28)	1.36(1)	C(25)−C(30)	1.54(1)	C(30)−C(31)	1.54(1)
C(30)−C(38)	1.49(2)	C(38)−N(1)	1.18(2)	C(30)−C(39)	1.48(2)
C(39)−N(2)	1.14(1)	C(34)−C(37)	1.56(2)	C(37)−C(40)	1.53(2)
C(40)−N(3)	1.12(2)	C(37)−C(41)	1.47(2)	C(41)−N(4)	1.13(2)
phenyl ring (C31−C36)	av 1.35				

Cl(1)−Rh(1)−P(1)	85.0(1)	Cl(1)−Rh(1)−O(1)	86.3(2)	P(1)−Rh(1)−O(1)	82.1(2)
Rh(1)−P(1)−C(23)	99.3(3)	P(1)−C(23)−C(24)	113.3(7)	C(23)−C(24)−O(2)	122.3(9)
Rh(1)−O(1)−C(24)	118.5(6)	C(25)−C(30)−C(31)	112.1(8)	C(25)−C(30)−C(38)	108.6(8)
C(25)−C(30)−C(39)	110.2(9)	C(31)−C(30)−C(38)	112.4(9)	C(31)−C(30)−C(39)	107.1(8)
C(38)−C(30)−C(39)	106.3(9)	C(34)−C(37)−C(40)	111(1)	C(34)−C(37)−C(41)	111.7(9)
C(40)−C(37)−C(41)	108(1)	C(30)−C(38)−N(1)	177(1)	C(30)−C(39)−N(2)	176(1)
C(37)−C(40)−N(3)	179(1)	C(37)−C(41)−N(4)	177(1)		

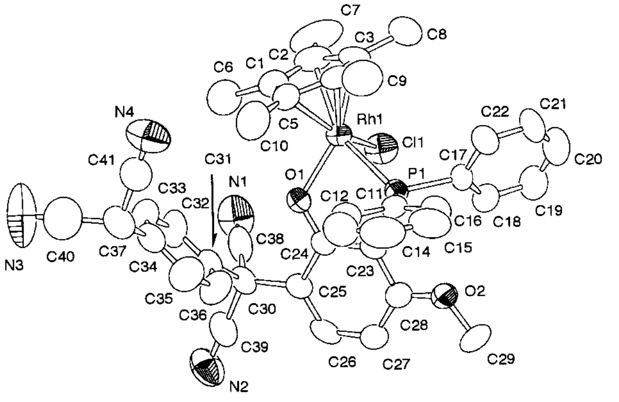

Figure 3. Perspective ORTEP view of the molecular structure of **4ad** with thermal ellipsoids drawn at 50% probability.

groups adopt a staggered conformation. The three angles around the Rh atom are 85.0° (Cl(1)−Rh(1)−P(1)), 86.3° (Cl(1)−Rh(1)−O(1)), and 82.1° (P(1)−Rh(1)−O(1)) and similar to those for **1a**, due to no Cl···H interaction.

When complexes **1a** and **1b** were treated with moderately electron withdrawing olefins such as fumalonitrile and dimethyl fumarate in methanol−CH_2Cl_2 at room temperature or at reflux, the starting materials were quantitatively formed. Similar treatment with Me_2−tcnq(**e**) failed to react.

Complex **2b** bearing a (*P*,*O*,*O*′) tridentate ligand was treated with 1 equiv of tcne at room temperature to give reddish orange crystals, formulated as [Cp*Ir(TDMPP-*P*,*O*,*O*′)(tcne)] **5bc** by FAB mass spectrometry. The IR spectrum showed a band at 2131 cm^{-1}, due to a C−N triple bond. The ^1H NMR spectrum showed four singlet resonances at δ 3.40, 3.45, 3.54, and 3.57, due to methoxy groups, which are nonequivalent. The H[C-

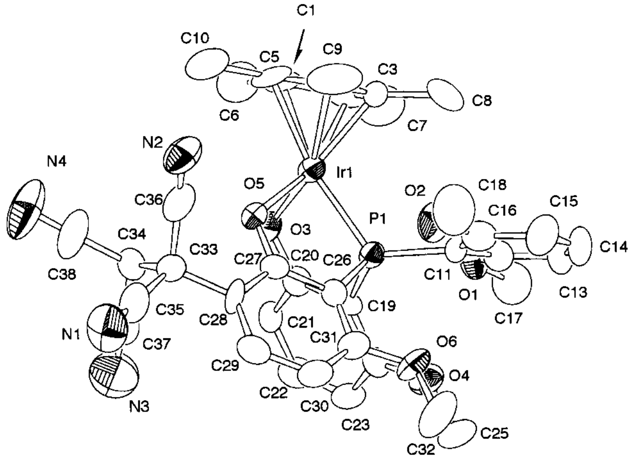

Figure 4. Perspective ORTEP view of the molecular structure of **5bc**·H_2O with thermal ellipsoids drawn at 50% probability. An H_2O molecule was omitted for clarity.

$(CN)_2]$ proton of δ 6.50 appeared at δ ca. 0.2 lower field than that for **3**. The $^{31}P\{^1H\}$ NMR spectrum showed a singlet at δ 15.9. The spectroscopic results suggested that **5bc** is a single insertion product arising from insertion of tcne into the C−H bond adjacent to the Ir−O bond. Indeed, X-ray crystal structure analysis verified the structure (Figure 4 and Table 5). The crystal contains a H_2O molecule as a crystal solvent. The molecule consists of two five-membered rings, Ir(1)-P(1)O(3)C(19)C(20) and Ir(1)P(1)O(5)C(26)C(27), which have a dihedral angle of 88.4(3)°. The O(3)···O(5) was separated by 2.83 Å. The $CH(CN)_2$ and $C(CN)_2R$ groups adopt a staggered conformation. The $HC(CN)_2C(CN)_2$ moiety is pointing in the same direction as the O(3) atom, as found in the C(27)−C(28)−C(33)−C(34) torsion angle of bond of −62(1)°. The Ir(1)−P(1) length of 2.272-(4) Å is ca. 0.01 Å shorter than that for **2b**, but the

Table 5. Selected Bond Lengths (Å) and Angles (deg) for 5bc·H_2O

Ir(1)−P(1)	2.272(4)	Ir(1)−O(3)	2.095(10)	Ir(1)−O(5)	2.108(10)
P(1)−C(19)	1.82(1)	C(19)−C(20)	1.37(2)	O(3)−C(20)	1.36(2)
P(1)−C(26)	1.81(2)	C(26)−C(27)	1.41(2)	O(5)−C(27)	1.32(2)
C(28)−C(33)	1.51(2)	C(33)−C(34)	1.56(2)	C(33)−(C35)	1.52(2)
C(35)−N(1)	1.09(2)	C(33)−C(36)	1.52(2)	C(36)−N(2)	1.12(2)
C(34)−C(37)	1.46(3)	C(37)−N(3)	1.14(2)	C(34)−C(38)	1.43(2)
C(38)−N(4)	1.16(2)				
O(1)···O(4)	2.91	O(2)···O(6)	3.15	O(3)···O(5)	2.83
O(4)···O(6)	2.93				
P(1)−Ir(1)−O(3)	82.3(3)	P(1)−Ir(1)−O(5)	81.2(3)	O(3)−Ir(1)−O(5)	84.8(4)
Ir(1)−P−C(19)	101.7(5)	P(1)−C(19)−C(20)	112(1)	C(19)−C(20)−O(3)	123(1)
Ir(1)−O(3)−C(20)	118.1(8)	Ir(1)−P(1)−C(26)	103.2(5)	P(1)−C(26)−C(27)	110(1)
C(26)−C(27)−O(5)	123(1)	Ir(1)−O(5)−C(27)	119.7(10)	C(19)−P(1)−C(26)	102.1(6)
C(28)−C(33)−C(34)	113(1)	C(28)−C(33)−C(35)	110(1)	C(28)−C(33)−C(36)	108(1)
C(34)−C(33)−C(35)	108(1)	C(34)−C(33)−C(36)	108(1)	C(35)−C(33)−C(36)	106(1)
C(33)−C(34)−C(37)	111(1)	C(33)−C(34)−C(38)	114(1)	C(37)−C(34)−C(38)	111(1)
C(33)−C(35)−N(1)	179(2)	C(33)−C(36)−N(2)	177(1)	C(34)−C(37)−N(3)	171(2)
C(34)−C(38)−N(4)	176(2)				

Table 6. Selected Bond Lengths (Å) and Angles (deg) for 7bc·0.5CH_2Cl_2

Ir(1)−P	2.277(2)	Ir(1)−O(1)	2.095(6)	Ir(1)−O(3)	2.097(6)
P(1)−C(101)	1.811(9)	C(101)−C(102)	1.41(1)	O(1)−C(102)	1.31(1)
P(1)−C(201)	1.814(9)	C(201)−C(202)	1.42(1)	O(3)−C(202)	1.31(1)
C(11)−C(103)	1.53(1)	C(11)−C(12)	1.59(1)	C(11)−C(13)	1.47(1)
C(13)−N(1)	1.12(1)	C(11)−C(14)	1.47(2)	C(14)−N(2)	1.14(1)
C(12)−C(15)	1.45(2)	C(15)−N(3)	1.17(2)	C(12)−C(16)	1.51(2)
C(16)−N(4)	1.12(2)	C(21)−C(203)	1.52(1)	C(21)−C(22)	1.60(1)
C(21)−C(23)	1.49(1)	C(23)−N(5)	1.11(1)	C(21)−C(24)	1.48(1)
C(24)−N(6)	1.14(1)	C(22)−C(25)	1.47(1)	C(25)−N(7)	1.13(1)
C(22)−C(26)	1.47(1)	C(26)−N(8)	1.15(1)		
C(12)−H(1)	1.18	C(22)−H(2)	1.10		
P(1)−Ir(1)−O(1)	82.7(2)	P(1)−Ir(1)−O(3)	79.9(2)	O(1)−Ir(1)−O(3)	85.3(2)
Ir(1)−P(1)−C(101)	101.6(3)	P(1)−C(101)−C(102)	119.0(9)	C(101)−C(102)−O(1)	123.2(9)
Ir(1)−O(1)−C(102)	119.5(6)	Ir(1)−P(1)−C(201)	103.6(3)	P(1)−C(201)−C(202)	108.7(6)
C(201)−C(202)−O(3)	118.6(8)	Ir(1)−O(3)−C(202)	121.0(5)	C(101)−P(1)−C(201)	99.9(4)
C(103)−C(11)−C(12)	106.2(8)	C(103)−C(11)−C(13)	111.7(9)	C(103)−C(11)−C(14)	112.2(8)
C(12)−C(11)−C(13)	108.7(9)	C(12)−C(11)−C(14)	108.3(9)	C(13)−C(11)−C(14)	109.6(9)
C(11)−C(12)−C(15)	112(1)	C(11)−C(12)−C(16)	112.4(9)	C(15)−C(12)−C(16)	108.0(10)
C(11)−C(13)−N(1)	178(1)	C(11)−C(14)−N(2)	176(1)	C(12)−C(15)−N(3)	178(1)
C(12)−C(16)−N(4)	178(1)	C(103)−C(11)−C(12)	106.2(8)	C(103)−C(11)−C(13)	111.7(9)
C(203)−C(21)−C(22)	109.4(7)	C(22)−C(21)-C(33)	108.3(7)	C(22)−C(23)−C(24)	106.3(7)
C(23)−C(21)−C(24)	109.6(8)	C(21)−C(22)−C(25)	109.8(7)	C(21)−C(22)−C(66)	111.8(8)
C(25)−C(22)−C(26)	112.6(8)	C(21)−C(23)−N(5)	177(1)	C(21)−C(24)−N(6)	179(1)
C(22)−C(25)−N(7)	175(1)	C(22)−C(26)−N(8)	175(1)	C(15)−C(12)−H(1)	122.9
C(16)−C(12)−H(1)	102.6	C(25)−C(22)−H(2)	102.3	C(26)−C(22)−H(2)	111.6

average Ir−O length is 0.03 Å longer than that for **2b**.[6] The Ir(1)−O(5) length is 0.01 Å longer than the Ir(1)−O(3) one, relieving steric repulsion with the $HC(CN)_2C(CN)_2$ moiety. The angles around the Ir atom are not different from those for **2b**. The C(33)−C(34) bond length of 1.56(2) Å is a conventional C−C single bond. Complex **2b** also reacted with 1 equiv of tcnq to form the 1:1 adduct **6bd**. The ^1H NMR spectrum showed four singlet resonances at δ 3.43, 3.44, 3.52, and 3.54 due to methoxy groups and a singlet at δ 5.17 due to $H[C(CN)_2]$ proton. The $^{31}P\{^1H\}$ NMR spectrum showed a singlet at δ 18.3. Reaction of **2b** with Me_2-tcnq (**e**) gave the 1:1 adduct **6be** based on FAB mass spectrometry, different from the case of the reaction with **1b**. The spectroscopic data are in good agreement with the structure.

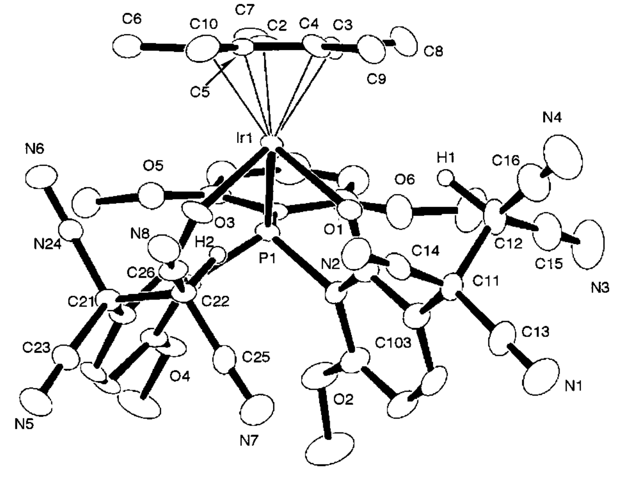

Figure 5. Perspective ORTEP view of the molecular structure of **7bc**·0.5CH_2Cl_2 with thermal ellipsoids drawn at 50% probability. A CH_2Cl_2 molecule was omitted for clarity.

When **2b** was treated with 2 equiv of tcne or tcnq, the 1:2 adducts formulated as [Cp*IrCl(TDMPP-*P*,*O*,*O*′)-$(L)_2$] (**7bc**: L = tcne; **8bd**: L = tcnq) were obtained. The IR spectra showed bands at 2250 cm^{-1} for **7bc** and at 2135 cm^{-1} for **8bd**. The ^1H NMR spectra showed two singlets around δ 3.5 due to methoxy protons, suggesting a symmetric structure. Indeed, X-ray structure analysis of **7bc** revealed that insertion of tcne occurred at two C−H positions adjacent to the Ir−O bonds (Figure 5). The $H(2)C(22)(CN)_2C(21)(CN)_2$ and $H(1)C(12)(CN)_2C(1)(CN)_2$ moieties are pointing in the same direction, relieving steric repulsion between the two groups. There are no significant differences in bond lengths and angles between **5bc** and **7bc**.

Scheme 2. Possible Route of Formation of 8bd

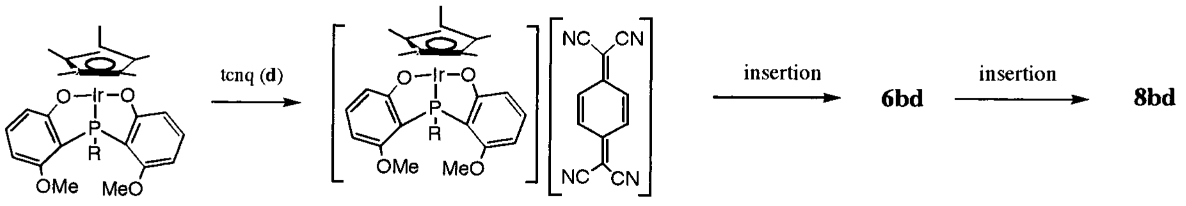

To examine a possible reaction path, the reaction of **5bc** with tcne was carried out. Addition of tcne to an orange solution of **5bc** gave **7bc** without a remarkable change of color. This suggested that the reaction of **2b** with tcne proceeded through stepwise insertion.

It has been observed that on addition of tcnq to a solution of **2b**, the mixture changed from yellow to pale green, and finally became yellow-orange to form **6bd** or **8bd**. This color change of the solution suggested the formation of a charge-transfer complex. Attempts to isolate a complex were unsuccessful. Thus, the solvent was removed from the pale green solution. The IR spectrum of the green residue showed two bands at 2180 and 2130 cm^{-1}, which is lower in energy than that (2222 cm^{-1}) for free tcnq and that (2209, 2180 cm^{-1}) of Li(tcnq). The electronic spectrum appeared at λ_{max} 851 and 751 nm, in agreement with that of Li(tcnq). These spectroscopic data are also in good agreement with those of [Cp*Ir(MDMPP-*P*,*O*)][tcnq], with bands at 2191 and 2137 cm^{-1} in the IR spectrum and absorption bands at λ_{max} 853 and 768 nm in the electronic spectrum, derived from the reaction of **1b** with Li(tcnq). On the basis of similarity of spectroscopic data, the green solid is considered to be a weak charge-transfer intermediate, [**2b**][tcnq] (Scheme 2).

These results suggest that the reaction with tcnq consists of an initial formation of a charge-transfer complex and proceeds with the electrophilic substitution of tceq to the activated aromatic ring, leading to the formal insertion of olefin. This reaction was accompanied by stepwise insertion of olefin into the C−H bond. However, since no green color species reminiscent of a charge-transfer complex were observed in the reactions with tcne, the reaction proceeds with the direct electrophilic substitution to the aromatic ring of the (*P*,*O*) bidentate or (*P*,*O*,*O*′) tridentate ligands.

These reactions demonstrate the novel C−H bond activation of aromatic rings in organometallic complexes in connection with insertion reactions of strongly electron withdrawing cyanoolefins.

Experimental Section

General Methods. All complexes were prepared under nitrogen atmosphere. Solvents were distilled under nitrogen prior to use with diethyl ether distilled from $LiAlH_4$ and methylene chloride distilled from CaH_2. Phosphines (MDMPP and TDMPP)[1b] and their pentamethylcyclopentadienyl complexes of rhodium[5] and iridium[6] were prepared according to the literature. The infrared and electronic absorption spectra were measured on FT/IR-5300 and U-best 30 spectrometers, respectively. NMR spectrometry was carried out on a Bruker AC250. ^{1}H NMR spectra were measured at 250 MHz, and ^{31}P-{^{1}H} NMR spectra were measured at 100 MHz using 85% H_3PO_4 as an external reference.

Reaction of 1a with tcne. To a solution of **1a** (53.2 mg, 0.092 mmol) in CH_2Cl_2 (10 mL) was added tcne (13 mg, 0.010 mmol) at room temperature. After 4 h, the solvent was removed and the solid was washed with diethyl ether. The residue was crystallized from CH_2Cl_2 and diethyl ether to give orange-brown crystals of **3ac** (43.6 mg, 66.3%). IR (Nujol): 2250 cm^{-1}. UV/vis (CH_2Cl_2): λ_{max} 392, 329 nm. ^{1}H NMR (250 MHz, $CDCl_3$): δ 1.50 (d, J_{PH} = 5.0 Hz, Cp*), 3.48 (s, OMe), 5.27 (s, CH_2Cl_2), 6.36 (s, CH), ca. 6.06 and 7.3−8.0 (c, ArH). ^{31}P NMR (100 MHz, $CDCl_3$): δ 45.2 (d, J_{RhP} = 142.7 Hz). FAB mass: *m*/*z*: 709 [M]$^+$, 673 [M − Cl]$^+$. Anal. Calcd for $C_{35}H_{31}N_4O_2PClRh{\cdot}CH_2Cl_2$: C, 54.46; H, 4.19; N, 7.06. Found: C, 54.87; H, 4.08; N, 6.84.

Analogously, yellow crystals of iridium complex **3bc** (42 mg, 43%) was obtained from **1b** (80 mg, 0.121 mmol) and tcne (21.8 mg, 0.170 mmol) according to a precedure similar to **1a**. UV/vis (CH_2Cl_2): λ_{max} 324 nm. ^{1}H NMR (250 MHz, $CDCl_3$): δ 1.53 (s, Cp*), 3.50 (s, OMe), 5.24 (s, CH_2Cl_2), 6.31 (s, $HC(CN)_2$), ca. 6.13 and 7.2−7.9 (c, ArH). ^{31}P NMR (100 MHz, $CDCl_3$): δ 26.2 (s). FAB mass: *m*/*z* 798 [M]$^+$. Anal. Calcd for $C_{35}H_{31}N_4O_2PClIr{\cdot}CH_2Cl_2$: C, 48.96; H, 3.77; N, 6.34. Found: C, 49.24; H, 3.83; N, 6.54.

Reaction of 1a with tcnq. Orange crystals **4ad** (28 mg, 32%) were obtained from **1a** (60 mg, 0.103 mmol) and tcnq (25 mg, 0.13 mol) by a procedure similar to **3ac**. IR (Nujol): 2247 cm^{-1}. UV/vis (CH_2Cl_2): λ_{max} 398, 330 nm. ^{1}H NMR (250 MHz, $CDCl_3$): δ 1.35 (d, J_{PH} = 3.0 Hz, Cp*, 15H), 3.44 (s, OMe, 3H), 5.08 (s, CH, 1H), 7.51 (AB q, *J* = 10.0 Hz, 4H), ca. 6.00 and 7.3−8.0 (c, ArH). ^{31}P NMR (100 MHz, $CDCl_3$): δ 48.4 (d, J_{RhP} = 150.0 Hz). FAB mass: *m*/*z* 785 [M]$^+$, 750 [M$^+$ − Cl]. Anal. Calcd for $C_{41}H_{35}N_4O_2PClRh$: C, 62.73; H, 4.49; N, 7.14. Found: C, 62.55; H, 4.55; N, 7.29.

Analogously, orange crystals of iridium complex **4bd** (63%) were obtained from **1b** and tcnq according to a precedure similar to **4ad**. IR (Nujol): 2145 cm^{-1}. UV/vis (CH_2Cl_2): λ_{max} 398 nm. ^{1}H NMR (250 MHz, $CDCl_3$): δ 1.41 (s, Cp*), 3.45 (s, OMe), 5.35 (s, CH_2Cl_2), 5.06 (s, $HC(CN)_2$), ca. 6.0 and 7.2−7.9 (c, ArH). ^{31}P NMR (100 MHz, $CDCl_3$): δ 28.1 (s). FAB mass: *m*/*z* 874 [M]$^+$, 839 [M − Cl]$^+$. Anal. Calcd for $C_{41}H_{35}N_4O_2PClIr{\cdot}0.25CH_2Cl_2$: C, 55.32; H, 4.00; N, 6.26. Found: C, 55.36; H, 4.11; N, 6.02.

Reaction of 2b with tcne in a 1:1 Ratio. To a solution of **2b** (79.8 mg, 0.11 mmol) in CH_2Cl_2 (10 mL) was added tcne (21.5 mg, 0.17 mmol) at room temperature. After stirring for 3 h, removal of the solvent and the crystallization of the residue from CH_2Cl_2 and diethyl ether gave reddish orange crystals of **5bc** (40.1 mg, 42.3%). IR (Nujol): 2131 cm^{-1}. ^{1}H NMR (250 MHz, $CDCl_3$): δ 1.54 (d, J_{PH} = 3.0 Hz, Cp*, 15H), 3.40 (s, OMe, 3H), 3.45 (s, OMe, 3H), 3.54 (s, OMe, 3H), 3.57 (s, OMe, 3H), 5.27 (s, CH_2Cl_2), 6.50 (s, CH), and 5.8−7.4 (c, ArH, 8H). ^{31}P NMR (100 MHz, $CDCl_3$): δ 19.5 (s). FAB mass: *m*/*z*: 867 [M]$^+$, 832 [M − Cl]$^+$. Anal. Calcd for $C_{38}H_{36}N_4O_8PIr{\cdot}0.5CH_2Cl_2$: C, 50.79; H, 4.10; N, 6.15. Found: C, 50.72; H, 4.22; N, 6.19. Complex **6bd** (71 mg, 68.4%) was obtained from the reaction of **2b** (80 mg, 0.11 mol) with tcnq (30 mg, 0.16 mmol) by a procedure similar to **5bc**. IR (Nujol): 2131 cm^{-1}. ^{1}H NMR (250 MHz, $CDCl_3$): δ 1.44 (d, J_{PH} = 1.8 Hz, Cp*, 15H), 3.43 (s, OMe, 3H), 3.44 (s, OMe, 3H), 3.52 (s, OMe, 3H), 3.55 (s, OMe, 3H), 5.17 (s, CH), and 6.0−8.0 (c, ArH, 9H). ^{31}P NMR (100 MHz, $CDCl_3$): δ 18.3 (s). Anal. Calcd for $C_{44}H_{40}N_4O_6PIr$: C, 55.98; H, 4.27; N, 5.94. Found: C, 55.77; H, 4.22; N, 6.11. Complex **6be** (53%) was obtained by the reaction between **2b**

and Me$_2$-tcnq (**e**). IR(Nujol): 2247 cm^{-1}. ^{1}H NMR (250 MHz, CDCl$_3$): δ 1.42 (d, $J_{PH} = 1.8$ Hz, Cp*, 15H), 2.36 (s, Me, 3H), 2.43 (s, Me, 3H), 3.44 (s, OMe, 3H), 3.48 (s, OMe, 3H), 3.56 (s, OMe, 3H), 3.57 (s, OMe, 3H), 5.03 (s, CH, 1H), 5.27 (s, CH$_2$Cl$_2$) and 5.7−7.5 (c, ArH, 10H). ^{31}P NMR (100 MHz, CDCl$_3$): δ 17.5 (s). FAB mass: m/z 867 [M]$^+$, 832 [M − Cl]$^+$. Anal. Calcd for $C_{46}H_{44}N_4O_8PIr\cdot0.5CH_2Cl_2$: C, 55.05; H, 4.56; N, 5.76. Found: C, 54.49; H, 4.52; N, 5.78.

Reaction of 2b with tcne in a 1:2 Ratio. To a solution of **2b** (79.8 mg, 0.11 mmol) in CH$_2$Cl$_2$ (10 mL) was added tcne (40.7 mg, 0.32 mmol) at room temperature. After stirring for 3 h, the solvent was removed and the residue was crystallized from CH$_2$Cl$_2$ and diethyl ether to give dark green crystals of **7bc** (42 mg, 44.8%). IR (Nujol): 2135 cm^{-1}. ^{1}H NMR (250 MHz, CDCl$_3$): δ 1.59 (d, $J_{PH} = 1.8$ Hz, Cp*, 15H), 3.47 (s, OMe, 6H), 3.60 (s, OMe, 6H), 5.27 (s, CH$_2$Cl$_2$), 6.28 (s, CH, 1H), and 6.0−8.0 (c, ArH, 9H). ^{31}P NMR (100 MHz, CDCl$_3$): δ 19.7 (s). FAB mass: m/z 996 [M + 1]$^+$, 929 [M − HC(CN)$_2$]$^+$, 865 [M − H$_2$-TCNE]$^+$. Anal. Calcd for $C_{44}H_{36}N_8O_6PIr\cdot0.5CH_2Cl_2$: C, 51.46; H, 3.59; N, 10.76. Found: C, 51.77; H, 3.74; N, 10.90.

Reaction of 2b with tcnq in a 1:2 Ratio. To a solution of **2b** (80 mg, 0.11 mmol) in CH$_2$Cl$_2$ (10 mL) was added tcnq (52 mg, 0.27 mmol) at room temperature. After stirring for 3 h, the solvent was removed and the residue was crystallized from CH$_2$Cl$_2$ and diethyl ether to give orange crystals of **8bd** (85.3 mg, 67.5%). IR (Nujol): 2250 cm^{-1}. ^{1}H NMR (250 MHz, CDCl$_3$): δ 1.41 (d, $J_{PH} = 1.8$ Hz, Cp*, 15H), 3.42 (s, OMe, 6H), 3.55 (s, OMe, 6H), 5.15 (s, CH), 5.27 (s, CH$_2$Cl$_2$) and 6.0−8.0 (c, ArH, 7H). ^{31}P NMR (100 MHz, CDCl$_3$): δ 18.7 (s). FAB mass: m/z 1148 [M]$^+$. Anal. Calcd for $C_{56}H_{44}N_8O_6PIr\cdot0.5CH_2Cl_2$: C, 56.99; H, 3.81; N, 9.41. Found: C, 56.53; H, 3.91; N, 8.70.

Reaction of 6bd with tcnq. To a solution of **6bd** (45 mg, 0.048 mol) in CH$_2$Cl$_2$ (10 mL) was added tcnq (mg, mol) at room temperature, and the mixture was stirred for 3 h. The solvent was removed and the residue was crystallized from CH$_2$Cl$_2$ and diethyl ether to form orange crystals of **8bd** (35 mg, 64%).

Reaction of 1b with Li[tcnq]. To a solution of **1b** (40 mg, 0.06 mmol) in CH$_2$Cl$_2$ (10 mL) was added Li[tcnq] (15 mg, 0.07 mmol) at room temperature. After 3 h, the mixture was filtered, the solvent was concentrated from the filtrate, and the residue was crystallized from CH$_2$Cl$_2$ and diethyl ether to give pale green complex [Cp*Ir(MDMPP-*P*,*O*)(tcnq)] (34 mg, 67.5%). IR (Nujol): 2191, 2137 cm^{-1}. UV−vis (CH$_2$Cl$_2$): 853, 768 nm. ^{1}H NMR (250 MHz, CDCl$_3$): δ 1.57 (bs, Cp*, 15H), 3.39 (bs, OMe, 3H), 4.27 (s, CH$_2$Cl$_2$), and 6.0−8.0 (c, ArH, 17H). ^{31}P NMR (100 MHz, CDCl$_3$): δ 69.4 (s). FAB mass: m/z 635 [[Cp*Ir(MDMPP-*P*,*O*)] + 1]$^+$. Anal. Calcd for $C_{41}H_{35}N_4O_2PIr\cdot CH_2Cl_2$: C, 54.60; H, 4.04; N, 6.06. Found: C, 54.89; H, 4.20; N, 6.08.

Data Collection. Complexes **3ac**·CH$_2$Cl$_2$, **3bc**, **4ad**, **5bc**·H$_2$O, and **7bc**·0.5CH$_2$Cl$_2$ were recrystallized from CH$_2$Cl$_2$/hexane or CH$_2$Cl$_2$/ether. Cell constants were determined from 20−25 reflections on a Rigaku AFC5S four-circle automated diffractometer. The crystal parameters along with data collections are summarized in Table 1. Data collection was carried out by a Rigaku AFC5S refractometer at 27 °C except a AFC7R diffractometer at −118 °C was used for **7bc**·0.5CH$_2$Cl$_2$. Intensities were measured by the $2\theta-\omega$ scan method using Mo Kα radiation ($\lambda = 0.71069$ Å). Throughout the data collection the intensities of the three standard reflections were measured every 150 or 200 reflections as a check of the stability of the crystals, and no decay was observed. Intensities were corrected for Lorentz and polarization effects. The absorption correction was made. Atomic scattering factors were taken from Cromer and Waber with the usual tabulation.[12] Anomalous dispersion effects were included in F_{calc};[16] the values of $\Delta f'$ and $\Delta f''$ were those of Creagh and McAuley.[13] All calculations were performed using the teXsan crytallographic software package.[14]

Determination of the Structures. The structures except **7bc**·0.5CH$_2$Cl$_2$, which was solved by direct methods, were solved by Patterson methods (DIRDIF92, PATTY).

The positions of all non-hydrogen atoms except the non-hydrogen atoms of a CH$_2$Cl$_2$ crystal solvent in **3ac**·CH$_2$Cl$_2$ were refined with anisotropic thermal parameters by using full-matrix least-squares methods. All hydrogen atoms of other complexes except hydrogen atoms H1 and H2 of **7bc**·0.5CH$_2$Cl$_2$, which were determined by difference Fourier syntheses, were calculated at the ideal positions with the C−H distance of 0.95 Å. Final difference Fourier syntheses showed peaks at heights up to 0.41−0.61 e A^{-3}.

Acknowledgment. We thank Professor Shigetoshi Takahashi and Dr Fumie Takei of The Institute of Scientific and Industrial Research, Osaka University, for measurements of FAB mass spectrometry.

Supporting Information Available: Tables of atomic coordinates and equivalent isotropic parameters, hydrogen coordinates, and isotropic displacement parameters for **3ac**·CH$_2$Cl$_2$, **3bc**, **4ad**, **5bc**·H$_2$O, and **7bc**·0.5CH$_2$Cl$_2$. The CCDC numbers of **3bc** and **4ad** are 103207 and 103208, respectively. This material is available free of charge via the Internet at http://pubs.acs.org.

OM000781C

---

(12) Cromer, D. T.; Waber, J. T. *International Tables for X-ray Crystallography*, Vol. IV; The Kynoch Press: Birmingham, England, 1974; Table 2.2A.

(13) Ibers, J. A.; Hamilton, W. C. *Acta Crystallogr.* **1964**, *17*, 781.

(14) Creagh, D. C.; McAuley, W. J. In *International Tables for Crystallography*, Vol. C; Wilson, A. J. C., Ed.; Kluwer Academic Publishers: Boston, 1992; Table 4.2.6.8, pp 219−222 .

(15) *teXsan*, Crystal Structure Analysis Package; Molecular Structure Corporation: 1985 & 1992.